EFFICIENT LARGE-SIGNAL FET PARAMETER EXTRACTION USING HARMONICS

OSA-89-MT-13-R

April 5, 1989

EFFICIENT LARGE-SIGNAL FET PARAMETER EXTRACTION USING HARMONICS

John W. Bandler, Fellow, IEEE, Qi-Jun Zhang, Member, IEEE,
Shen Ye, Student Member, IEEE, and Shao Hua Chen, Member, IEEE

Abstract We present a novel approach to nonlinear large-signal FET model parameter extraction for GaAs MESFET devices measured under large-signal conditions. Powerful nonlinear adjoint-based optimization, which employs the harmonic balance method as the nonlinear circuit simulation technique, simultaneously processes multi-bias, multi-power-input, multi-fundamental-frequency excitations and multi-harmonic measurements to uniquely reveal the parameters of the intrinsic FET. Different from other methods by which the model parameters are extracted using DC and small-signal measurements, our new approach can provide more accurate and reliable large-signal model parameters extracted under actual operating conditions. The modified Materka and Kacprzak FET model serves as an example. Numerical results verify that our approach can effectively determine the parameters of this model. Including harmonics in parameter extraction results in a reliable large-signal model. Real data provided by Texas Instruments has also been employed. The technique has been implemented in a new program called HarPE (Harmonic balance driven model Parameter Extractor).

This work was supported in part by Optimization Systems Associates Inc. and in part by the Natural Sciences and Engineering Research Council of Canada under Grant A7239.

J.W. Bandler, Q.J. Zhang and S.H. Chen are with Optimization Systems Associates Inc., P.O. Box 8083, Dundas, Ontario, Canada L9H 5E7. J.W. Bandler is also with and S. Ye is with the Simulation Optimization Systems Research Laboratory and the Department of Electrical and Computer Engineering, McMaster University, Hamilton, Canada L8S 4L7.

I. INTRODUCTION

An accurate nonlinear large-signal FET model is critical to nonlinear microwave CAD. Various approaches to FET modeling have been proposed, e.g., [1-4]. The dominant nonlinear bias-dependent current source, namely, the drain-to-source current source, in these models is commonly determined by fitting static or dynamic DC I-V characteristics only [1, 2, 4-6], or by matching DC characteristics and small-signal S-parameters simultaneously [3]. Other nonlinear elements in the model are either determined by applying special DC biases such as to determine the parameters of the gate-to-source nonlinear current source in the Materka and Kacprzak model [2], or by using small-signal S-parameters such as to determine the gate-to-source nonlinear capacitor [3].

The FET models obtained by those methods may provide accurate results under DC and/or small-signal operating conditions. They may not, however, be accurate enough for high-frequency large-signal applications [7], since they are determined under small-signal conditions and then used to predict the behaviour for large-signal operations.

In this paper, we present, for the first time, a truly nonlinear large-signal FET parameter extraction procedure which utilizes spectrum measurements, including DC bias information and power output at different harmonics under practical working conditions [8]. Besides multi-bias and multi-frequency excitations, multi-power-input is introduced for large-signal parameter extraction. The harmonic balance method [9] is employed for fast nonlinear frequency domain simulation in conjunction with ℓ_1 and ℓ_2 optimization for extracting the parameters of the nonlinear elements in the large-signal FET model. Powerful nonlinear adjoint analysis for sensitivity computation [10] is implemented with attendant advantages in computation time.

Numerical experiments show that all the parameters can be identified under practical large-signal conditions, and that including higher harmonics in large-signal parameter extraction is crucial to the reliability of the model. Numerical results are also obtained in processing actual measurement data provided by Texas Instruments. Good agreement between the measurements

and the model responses is reached, demonstrating the feasibility of our new parameter extraction approach.

In Section II, the formulation of the large-signal parameter extraction optimization problem is presented. Section III describes the applications of the harmonic balance technique to model response simulations and nonlinear adjoint sensitivity analysis to gradient calculations. An automatic weight assignment algorithm enhancing parameter extraction optimization is given in Section IV. Numerical examples are discussed in Section V, where we use the modified Materka and Kacprzak FET model [11], which has 21 parameters characterizing the nonlinear intrinsic part of this large-signal FET model.

II. OPTIMIZATION FOR LARGE-SIGNAL PARAMETER EXTRACTION

Consider the FET model and its measurement environment shown in Fig. 1, where Y_{in} and Y_{out} are input and output 2-ports, Y_g and Y_d are gate and drain bias 2-ports, respectively. A large-signal power input P_{in} is applied to the circuit. The responses including DC and several harmonic components are measured.

In addition to the multi-bias, multi-frequency concept we pioneered for small-signal parameter extraction [3,12], we allow the circuit to be excited at several input power levels. Various combinations of bias points, fundamental frequencies and input power levels together with multi-harmonic measurements contribute to the information needed for real large-signal parameter extraction. In the following discussion we use the term bias-input-frequency combination to indicate the modeling circuit working at a bias point with a particular input power level and at a particular fundamental frequency.

Assume for the jth bias-input-frequency combination, j=1, 2, ... M, the measurement is

$$\mathbf{S}_j = [S_j(0) \quad S_j(\omega_{j1}) \quad \dots \quad S_j(\omega_{jH})]^T, \tag{1}$$

where M is the number of bias-input-frequency combinations, $S_j(0)$ is the DC component of the measurement, $S_j(\omega_{jk})$, k=1, 2, ..., H, are the kth harmonic components at the jth bias-input-

frequency combination, and H is the number of harmonics contained in the measurement. $S_j(0)$ can be taken as the bias-related DC voltage or current, which varies at different fundamental frequencies and input levels even at a fixed bias point. $S_j(\omega_{jk})$ is usually the output power [13]. (The equivalent output voltage with phase information might also be employed [8]).

Corresponding to (1), the model response $\mathbf{F}_j(\phi)$ can be expressed as

$$\mathbf{F}_j(\phi) = [F_j(\phi,0) \quad F_j(\phi,\omega_{j1}) \quad \ldots \quad F_j(\phi,\omega_{jH})]^T, \qquad (2)$$

$$j=1, 2, \ldots M,$$

where ϕ stands for the parameters of the model to be determined. The parameter extraction problem can be formulated as the following optimization problem

$$\min_{\phi} \sum_{j=1}^{M} (w_{jdc} \mid F_j(\phi,0) - S_j(0) \mid^p + \sum_{k=1}^{H} w_{jk} \mid F_j(\phi,\omega_{jk}) - S_j(\omega_{jk}) \mid^p), \qquad (3)$$

where w_{jdc} and w_{jk} are weighting factors, and p=1 or 2 corresponds to ℓ_1 or ℓ_2 optimization, respectively. The criterion of the above optimization is to match the model responses to the measurements at DC and several harmonics. It is clear that the practical usefulness of this parameter extraction approach depends on the effectiveness of calculating the model responses $F_j(\phi)$, j=1, 2, ..., M, and their derivatives. (In the next section we will show that the numerical computation of $F_j(\phi)$ and its derivatives is not a trivial task.)

The magnitude of the circuit responses varies widely at different bias-input-frequency combinations and different harmonics. An automatic weight assignment algorithm has been developed to improve robustness and enhance convergence speed. If the harmonic measurement is made in the form of output power, the conditioning of the optimization problem can be further improved by converting the output power to its equivalent output voltage.

III. NONLINEAR CIRCUIT SIMULATION AND GRADIENT CALCULATION

For a nonlinear large-signal FET model, the circuit model in Fig. 1 is nonlinear. This means that the model response $\mathbf{F}_j(\phi)$ in (2) must be obtained by solving a dynamic nonlinear

circuit, and the gradient of the objective function in (3) involves calculation of the derivatives of the dynamic nonlinear circuit response.

To solve these two difficult problems, we have employed the efficient harmonic balance method [9] for fast nonlinear circuit simulation in the frequency domain. Powerful nonlinear adjoint sensitivity analysis technique [10] has been implemented to calculate the derivatives of the model response and therefore the gradient of the objective function in (3) with respect to ϕ. In this section we discuss the applications of the harmonic balance technique to model response simulation, and nonlinear adjoint sensitivity analysis to gradient calculations.

Let the nonlinear circuit model be partitioned into linear and nonlinear subcircuits, as illustrated in Fig. 2. Assume that the multi-port Y matrix of the linear subcircuit can be established, all the nonlinear elements are voltage-controlled, and there is no nonlinear inductor inside the intrinsic FET model. Also, for simplicity, we assume that the parameters in the linear subcircuits are known. In the rest of this section, we will focus our discussions on the jth bias-input-frequency combination, therefore the corresponding subscript j will be omitted to simplify the notation. Other bias-input-frequency combinations can be treated similarly.

Nonlinear Circuit Simulation Using Harmonic Balance Method

Following [9], the harmonic balance equation for our model can be expressed as

$$\mathbf{I}_d(\phi,\mathbf{V}(\phi),\omega_k) + j\Omega(\omega_k)\mathbf{Q}(\phi,\mathbf{V}(\phi),\omega_k) + \mathbf{Y}(\omega_k)\mathbf{V}(\phi,\omega_k) + \mathbf{I}_s(\omega_k) = 0, \qquad (4)$$

$$k=0,\ 1,\ \ldots,\ H',$$

where k represents the kth harmonic, ω_0=0 corresponds to the DC component, $\mathbf{V}(\phi) = [\mathbf{V}^T(\phi,0)\ \mathbf{V}^T(\phi,\omega_1)\ \ldots\ \mathbf{V}^T(\phi,\omega_{H'})]^T$ is the voltage vector to be solved for, Y stands for the multi-port admittance matrix of the linear subcircuit, $\mathbf{I}_s$ is the equivalent current excitation from the external excitations, $\mathbf{I}_d$ corresponds to the current from the nonlinear current sources, $\Omega(\omega_k)$ is a diagonal matrix with ω_k as diagonal elements, and **Q** corresponds to the charge from the nonlinear capacitors. For example, $\mathbf{I}_d$ may contain the drain-to-source and drain-to-gate nonlinear current sources, and **Q** may include the gate-to-source nonlinear capacitor, etc.

In (4) ϕ represents the optimization variables, i.e., the parameters to be determined, and H′ the number of harmonics considered in the harmonic balance simulation. It should be noticed that H′ ≥ H (the number of measured harmonics used), and H′ can be different for different bias-input-frequency combinations. For higher accuracy H′ could be greater than H.

We solve (4) by organizing it into a scalar form

$$\begin{bmatrix} I_d^R(\phi,V(\phi),0) \\ I_d^R(\phi,V(\phi),\omega_1) \\ .. \\ .. \\ I_d^R(\phi,V(\phi),\omega_{H'}) \\ I_d^I(\phi,V(\phi),0) \\ I_d^I(\phi,V(\phi),\omega_1) \\ .. \\ .. \\ I_d^I(\phi,V(\phi),\omega_{H'}) \end{bmatrix} + \begin{bmatrix} & & & & -\Omega(0) & & & & \\ & & & & & -\Omega(\omega_1) & & & \\ & & & & & & .. & & \\ & & & & & & & .. & \\ & & & & & & & & -\Omega(\omega_{H'}) \\ \Omega(0) & & & & & & & & \\ & \Omega(\omega_1) & & & & & & & \\ & & .. & & & & & & \\ & & & .. & & & & & \\ & & & & \Omega(\omega_{H'}) & & & & \end{bmatrix} \begin{bmatrix} Q^R(\phi,V(\phi),0) \\ Q^R(\phi,V(\phi),\omega_1) \\ .. \\ .. \\ Q^R(\phi,V(\phi),\omega_{H'}) \\ Q^I(\phi,V(\phi),0) \\ Q^I(\phi,V(\phi),\omega_1) \\ .. \\ .. \\ Q^I(\phi,V(\phi),\omega_{H'}) \end{bmatrix}$$

$$+ \begin{bmatrix} Y^R(0) & & & & -Y^I(0) & & & & \\ & Y^R(\omega_1) & & & & -Y^I(\omega_1) & & & \\ & & .. & & & & .. & & \\ & & & .. & & & & .. & \\ & & & & Y^R(\omega_{H'}) & & & & -Y^I(\omega_{H'}) \\ Y^I(0) & & & & & Y^R(0) & & & \\ & Y^I(\omega_1) & & & & & Y^R(\omega_1) & & \\ & & .. & & & & & .. & \\ & & & .. & & & & & .. \\ & & & & Y^I(\omega_{H'}) & & & & Y^R(\omega_{H'}) \end{bmatrix} \begin{bmatrix} V^R(\phi,0) \\ V^R(\phi,\omega_1) \\ .. \\ .. \\ V^R(\phi,\omega_{H'}) \\ V^I(\phi,0) \\ V^I(\phi,\omega_1) \\ .. \\ .. \\ V^I(\phi,\omega_{H'}) \end{bmatrix} + \begin{bmatrix} I_s^R(0) \\ I_s^R(\omega_1) \\ .. \\ .. \\ I_s^R(\omega_{H'}) \\ I_s^I(0) \\ I_s^I(\omega_1) \\ .. \\ .. \\ I_s^I(\omega_{H'}) \end{bmatrix} = 0,$$

or, simply

$$\bar{I}_d(\phi,\bar{V}(\phi)) + \bar{\Omega}\bar{Q}(\phi,\bar{V}(\phi)) + \bar{Y}\bar{V}(\phi) + \bar{I}_s = 0, \tag{5}$$

where superscripts R and I represent real and imaginary parts of the corresponding component, respectively. Note that in solving the harmonic balance equation (5), ϕ is constant and $\bar{V}(\phi)$ is the variable. Powell's algorithm for solving nonlinear equations [14] is used, where in order to save computation time and provide higher accuracy the exact Jacobian matrix is calculated in our program, i.e.,

$$\bar{J}(\phi,\bar{V}(\phi)) = \left[\frac{\partial \bar{I}_d^T(\phi,\bar{V}(\phi))}{\partial \bar{V}(\phi)} + \bar{\Omega}^T \right] \left[\frac{\partial \bar{Q}^T(\phi,\bar{V}(\phi))}{\partial \bar{V}(\phi)} + \bar{Y}. \right]^T \tag{6}$$

The detailed calculations of the entries of $\bar{J}(\phi,\bar{V}(\phi))$ are discussed in [9].

When the solution $\overline{\mathbf{V}}(\boldsymbol{\phi})$ is reached, the model response $\mathbf{F}(\boldsymbol{\phi})$ can be easily obtained,

$$\mathbf{F}(\boldsymbol{\phi},\omega_k) = \mathbf{a}^T(\omega_k)\mathbf{V}(\boldsymbol{\phi},\omega_k) + \mathbf{b}^T(\omega_k)\mathbf{E}(\omega_k) \tag{7}$$

$$k=0,\ 1,\ \ldots,\ H,$$

where $\mathbf{a}(\omega_k)$ and $\mathbf{b}(\omega_k)$ are constant vectors determined by the linear subcircuit, and $\mathbf{E}(\omega_k)$ corresponds to the external excitations including power input source and bias sources.

Gradient Calculation by Nonlinear Adjoint Sensitivity Analysis

Let N be an index set indicating interfacing ports between linear and nonlinear parts, and $\mathbf{e}_{n1}(k)$ and $\mathbf{e}_{n2}(k)$ be such unit vectors that $V_n(\boldsymbol{\phi},\omega_k) = (\mathbf{e}_{n1}(k)+j\mathbf{e}_{n2}(k))^T\overline{\mathbf{V}}(\boldsymbol{\phi})$, $n\in N$. The circuit response $\mathbf{F}(\boldsymbol{\phi},\omega_k)$ in (7) can be rewritten as

$$\mathbf{F}(\boldsymbol{\phi},\omega_k) = \sum_{n\in N} a_n(\omega_k)(\mathbf{e}_{n1}(k) + j\mathbf{e}_{n2}(k))^T\overline{\mathbf{V}}(\boldsymbol{\phi}) + \mathbf{b}^T(\omega_k)\mathbf{E}(\omega_k). \tag{8}$$

The derivative of $\mathbf{F}(\boldsymbol{\phi},\omega_k)$ w.r.t. ϕ_i is then

$$\frac{\partial \mathbf{F}(\boldsymbol{\phi},\omega_k)}{\partial \phi_i} = \sum_{n\in N} a_n(\omega_k) \left[\mathbf{e}_{n1}^T(k) \frac{\partial \overline{\mathbf{V}}(\boldsymbol{\phi})}{\partial \phi_i} + j\mathbf{e}_{n2}^T(k) \frac{\partial \overline{\mathbf{V}}(\boldsymbol{\phi})}{\partial \phi_i} \right]. \tag{9}$$

To realize the above derivative, we first derive from (5) that

$$\frac{\partial \overline{\mathbf{V}}(\boldsymbol{\phi})}{\partial \phi_i} = -\overline{\mathbf{J}}^{-1}(\boldsymbol{\phi},\overline{\mathbf{V}}(\boldsymbol{\phi})) \left[\frac{\partial \overline{\mathbf{I}}_d(\boldsymbol{\phi},\overline{\mathbf{V}}(\boldsymbol{\phi}))}{\partial \phi_i} + \overline{\Omega} \frac{\partial \overline{\mathbf{Q}}(\boldsymbol{\phi},\overline{\mathbf{V}}(\boldsymbol{\phi}))}{\partial \phi_i} \right], \tag{10}$$

where $\overline{\mathbf{J}}(\boldsymbol{\phi},\overline{\mathbf{V}}(\boldsymbol{\phi}))$ is defined in (6) and is available at the solution of the harmonic balance equation. Then by multiplying both sides of equation (10) by $\mathbf{e}_{n1}^T(k)$, we get

$$\mathbf{e}_{n1}^T(k) \frac{\partial \overline{\mathbf{V}}(\boldsymbol{\phi})}{\partial \phi_i} = -\hat{\overline{\mathbf{V}}}^T(\boldsymbol{\phi}) \left[\frac{\partial \overline{\mathbf{I}}_d(\boldsymbol{\phi},\overline{\mathbf{V}}(\boldsymbol{\phi}))}{\partial \phi_i} + \overline{\Omega} \frac{\partial \overline{\mathbf{Q}}(\boldsymbol{\phi},\overline{\mathbf{V}}(\boldsymbol{\phi}))}{\partial \phi_i} \right] \tag{11}$$

where

$$\hat{\overline{\mathbf{V}}}^T(\boldsymbol{\phi}) = [(\hat{\mathbf{V}}^R(\boldsymbol{\phi},0))^T\ (\hat{\mathbf{V}}^R(\boldsymbol{\phi},\omega_1))^T\ \ldots\ (\hat{\mathbf{V}}^R(\boldsymbol{\phi},\omega_{H'}))^T\ (\hat{\mathbf{V}}^I(\boldsymbol{\phi},0))^T\ (\hat{\mathbf{V}}^I(\boldsymbol{\phi},\omega_1))^T\ \ldots\ (\hat{\mathbf{V}}^I(\boldsymbol{\phi},\omega_{H'}))^T]$$

and is determined by solving the adjoint system

$$\overline{\mathbf{J}}^T(\boldsymbol{\phi},\overline{\mathbf{V}}(\boldsymbol{\phi}))\ \hat{\overline{\mathbf{V}}}(\boldsymbol{\phi}) = \mathbf{e}_{n1}(k). \tag{12}$$

It can be proved that if ϕ_i is a parameter of a nonlinear element at branch b, then

$$\mathbf{e}_{n1}^{T}(k)\,\frac{\partial \bar{V}(\phi)}{\partial \phi_i} = \begin{cases} -\sum_{\ell=0}^{H'} \text{Real}[\hat{\bar{V}}_b(\phi,\omega_\ell)G^{*}_{bIi}(\phi,\omega_\ell)], & \text{if } b\in\{\text{nonlinear current sources}\} \\ -\sum_{\ell=0}^{H'} \text{Imag}[\hat{\bar{V}}_b(\phi,\omega_\ell)G^{*}_{bQi}(\phi,\omega_\ell)], & \text{if } b\in\{\text{nonlinear capacitors}\} \end{cases} \tag{13}$$

where the superscript * stands for complex conjugate, and $G_{bIi}(\phi,\omega_\ell)$ and $G_{bQi}(\phi,\omega_\ell)$ are the ℓth Fourier coefficients of the partial derivatives of the current $i_b(\phi,v(t))$ and charge $q_b(\phi,v(t))$ w.r.t. ϕ_i, respectively. See [10]. For example, if branch b is the gate-to-source diode with characteristics

$$i_b(\phi,v(t)) = I_{G0}[\exp(\alpha_G v_b(t)) - 1],$$

and $\phi_i=\alpha_G$, we will have

$$\frac{\partial i_b(\phi,v(t))}{\partial \phi_i} = I_{G0}v_b(t)\exp(\alpha_G v_b(t))$$

and

$$G_{bIi}(\phi,\omega_\ell) = \frac{1}{N_T}\sum_{m=0}^{N_T-1} \frac{\partial i_b(\phi,v(mT_1))}{\partial \phi_i} \exp(-j\ell m\cdot 2\pi/N_T),$$

where discrete Fourier transformation is used, $N_T\geq(2H'+1)$ is the number of samples in the time domain within one period T, $T_1=T/N_T$, and T=1/(fundamental frequency).

The same derivations can be applied to

$$\mathbf{e}_{n2}^{T}(k)\,\frac{\partial \bar{V}(\phi)}{\partial \phi_i}.$$

Hence, $\partial F(\phi,\omega_k)/\partial\phi_i$ in (9) can be obtained. Consequently, the gradient of the objective function in (3) can be obtained.

Summing up, we can see that the gradient of the nonlinear circuit response $F(\phi)$ w.r.t. ϕ can be calculated by nonlinear adjoint analysis which utilizes the existing Jacobian matrix from the solution of the harmonic balance equation to complete all the adjoint analysis. The equi-

valent conductances at the nonlinear element level, i.e., $G_{bIi}(\phi,\omega_\ell)$ or $G_{bQi}(\phi,\omega_\ell)$, are the same for different adjoint systems, and therefore only need to be calculated once. Compared with the perturbation method for gradient computations which requires solving one nonlinear circuit for each optimization variable, the nonlinear adjoint analysis not only provides the exact gradient of the objective function, but more importantly, it significantly reduces the computation time and makes our parameter extraction approach computationally practical [10,15].

IV. WEIGHT ASSIGNMENT PROCEDURE

In the large-signal parameter extraction approach presented in Section II, the model response is optimized to match several harmonics at various bias-input-frequency combinations. Two difficulties must be overcome to optimize the objective function in (3): the magnitude differences between different harmonic measurements, and the differences between different bias-input-frequency combinations. Suitably chosen weighting factors can balance these differences and improve the convergence of the optimization. This weight assignment procedure assumes that (a) the possibility of having large measurement errors is small, (b) the power measurement has been converted to the magnitude of the output voltage and (c) we want one harmonic in a bias-input-frequency combination to have the same opportunity in the objective function as the same harmonic in another bias-input-frequency combination.

Balance of a Harmonic Between Different Bias-Input-Frequency Combinations

In (1) of Section II, we have defined the kth harmonic measurement $S_j(\omega_{jk})$, where j=1, 2, ..., M corresponds to the jth bias-input-frequency combination. Let $\overline{S}_k$ be the mean value of the kth harmonic measurement over M combinations

$$\overline{S}_k = \frac{1}{M} \sum_{j=1}^{M} S_j(\omega_{jk}), \qquad (14)$$

$$k=0,\ 1,\ ...,\ H.$$

Since the measurement will not be zero, we can balance the kth harmonic by

$$w'_{jk} = \frac{\overline{S}_k}{S_j(\omega_{jk})}. \tag{15}$$

Minimum and maximum bounds can be imposed on w'_{jk}, i.e., simple interpolation adjustment can be used within the kth harmonic if some w'_{jk}, j=1, ..., M, lies outside the bound(s).

Balance Between Different Harmonics

In practice we may want to emphasize some harmonics over the others, e.g., the lower harmonic measurements may be emphasized due to their larger magnitudes and therefore higher measurement accuracy. This requires adjustment between different harmonics. Let K_k be the weight adjustment factor for the kth harmonic. Then the weighting factors for the optimization problem (3) can be expressed as

$$w_{jk} = K_k \, w'_{jk} \frac{\overline{S}_1}{\overline{S}_k}, \tag{16}$$

$$k=1, 2, ..., H$$

and

$$w_{jdc} = K_0 \, w'_{j0} \frac{\overline{S}_1}{\overline{S}_0}, \tag{17}$$

where we take the mean value of the first harmonic measurement as a reference. As an example, if we want to have equal emphasis on the DC and fundamental harmonic measurements and lower emphasis on higher harmonic measurement, we can choose $K_k=1$ for k=0 and 1, and $K_k=B^{-k}$ for k=2, ..., H where B>1.

V. NUMERICAL EXAMPLES

In the numerical examples, we use the Microwave Harmonica [11] modified Materka and Kacprzak FET model as the intrinsic FET, as shown in Fig. 3. All the linear FET model parameters such as the parasitics in Fig. 1 are extracted using small-signal measurement data.

The nonlinear elements of the model are described by [11]

$$i_D = F[v_G(t - \tau),\ v_D(t)]\ (1 + S_S \frac{v_D}{I_{DSS}}),$$

$$F(v_G,v_D)=I_{DSS}\left\{1 - \frac{v_G}{V_{p0} + \gamma v_D}\right\}^{(E + K_E v_G)} \cdot \tanh\left\{\frac{S_1 v_D}{I_{DSS}(1 - K_G v_G)}\right\},$$

$$i_G = I_{G0}\ [\exp(\alpha_G v_G) - 1],$$

$$i_B = I_{B0}\ \exp[\alpha_B(v_D - v_1 - V_{BC})],$$

$$\begin{cases} R_1 = R_{10}(1 - K_R v_G), \\ R_1 = 0, \quad \text{if } K_R v_G \geq 1, \end{cases} \tag{18}$$

$$\begin{cases} C_1 = C_{10}(1 - K_1 v_G)^{-1/2} + C_{1S}, \\ C_1 = C_{10}\sqrt{5} + C_{1S}, \quad \text{if } K_1 v_G \geq 0.8, \end{cases}$$

and

$$\begin{cases} C_F = C_{F0}[1 - K_F(v_1 - v_D)]^{-1/2}, \\ C_F = C_{F0}\sqrt{5}, \quad \text{if } K_F(v_1 - v_D) \geq 0.8, \end{cases}$$

where I_{DSS}, V_{P0}, γ, E, K_E, S_1, K_G, τ, S_S, I_{G0}, α_G, I_{B0}, α_B, V_{BC}, R_{10}, K_R, C_{10}, K_1, C_{1S}, C_{F0}, and K_F are the parameters to be determined. Since only one of I_{B0} and V_{BC} is independent, we fix V_{BC} and let

$$\phi = [I_{DSS}\ V_{P0}\ \gamma\ E\ K_E\ S_1\ K_G\ \tau\ S_s\ I_{G0}\ \alpha_G\ I_{B0}\ \alpha_B\ R_{10}\ K_R\ C_{10}\ K_1\ C_{1S}\ C_{F0}\ K_F]^T. \tag{19}$$

During the optimization the nonlinear circuit is solved using harmonic balance method, where the excitation of the circuit is the available input power P_{in} which can be converted to an equivalent input voltage source V_{in} by

$$P_{in} = \frac{|V_{in}|^2}{8 \cdot R_0}. \tag{20}$$

Three cases are discussed as follows. In Case 1, we will show the theoretical aspects of the proposed approach, i.e., the robustness, reliability and efficiency of our parameter extraction approach if there is no model deficiency. Case 2 gives a numerical experiment of matching the modified Materka and Kacprzak model to the Curtice model. In Case 3, we will discuss practical large-signal FET model parameter extraction for the measurement data provided by Texas Instruments.

Case 1: Robustness and Efficiency of the Parameter Extraction Approach

We use the values of the FET parasitics from [3]

$$[R_g\ L_g\ R_s\ L_s\ R_d\ L_d\ C_{ds}\ R_{de}\ C_{de}] = [0.0119\Omega\ 0.1257\text{nH}$$

$$0.3740\Omega\ 0.0107\text{nH}\ 0.0006\Omega\ 0.0719\text{nH}\ 0.1927\text{pF}\ 440\Omega\ 1.5\text{pF}],$$

and assume that the solution of the model is also from [3] which is listed in Table I. The circuit is simulated at four bias points: (V_{GB}=-0.5V, V_{DB}=2V), (V_{GB}=-2V, V_{DB}=2V), (V_{GB}=-0.5V, V_{DB}=5V), and (V_{GB}=-2V, V_{DB}=5V). At each bias point three input power levels (P_{in}=5, 10, and 15dBm), and two fundamental frequencies (f_1=1 and 2GHz) are applied, respectively. There are 24 bias-input-frequency combinations in total. Six harmonics are considered in the harmonic balance simulation. The output power P_{out} and the DC voltage V_{DC}, see Fig. 1, of the simulation results are then used as the simulated measurements. This corresponds to the situation of no model deficiencies.

To examine the robustness of the approach, we generated several starting points by uniformly perturbing the assumed solution by 20 to 40 percent and optimized them with the ℓ_1 norm, i.e., p=1 in (3). The circuit response $F_j(\phi)$ in (2) was computed using six harmonics (H'=6). In the case that there is no measurement error, i.e., the exact simulation results obtained at the assumed solution are used as the measurement data, all the starting points converged to the known solution exactly when we included the first three, two or one harmonics (plus DC) in the objective function, i.e., H=3, 2, or 1 in (3), respectively. However, it has been observed that the speed of convergence is usually faster when more harmonics are considered in the

optimization.

To simulate a real measurement environment we added 10% normally distributed random noise to the simulated measurements. The same starting points were optimized with the ℓ_2 norm, i.e., p=2 in (3), and the same conditions were tested. When H=3 or 2 in (3), all the starting points converged to virtually one solution which is close to the assumed solution and gave very good match to the measurement with noise. When H=1, however, those different starting points did not converge to a single solution close to the assumed solution. Though at these solutions, the matches to the measurements with noise at DC and fundamental harmonic are better compared with those achieved when H=3 or 2, poor matches at second, third and/or higher harmonics exist. Table II shows the match errors at one of the bias-input-frequency combinations at the solutions obtained when H=1, 2 and 3 in the objective function.

From these experiments, we can see that with our approach the nonlinear parameters can theoretically be determined even when H=1 in (3). In practice when the model is not perfect and the measurement contains error, it is necessary to include higher harmonic measurements in the nonlinear large-signal model parameter extraction, for it not only improves convergence, but more importantly, it results in a more reliable model.

Two different starting points were used to compare the CPU execution time with and without nonlinear adjoint analysis for gradient computation. To reach the ℓ_1 objective function value around 1.0×10^{-3} on another 16 bias-input-frequency combination parameter extraction case with 20 variables and 64 error functions, the Fortran program with the adjoint analysis runs approximately 10 times faster than that without adjoint analysis, (about 200 sec. vs 2000 sec. on a VAX 8650 computer.)

Case 2: Fitting to the Curtice Model

Here we use a set of data generated by the Curtice model [4]. The circuit is similar to that of Fig. 1 except that the intrinsic FET is replaced by the intrinsic part of the Curtice model. Some of the parameters of the Curtice model are taken from Fig. 13 of [4]. See Table

III. The parameters in the linear part of the circuit is the same as those in Case 1.

We selected 32 bias-input-frequency combinations, as shown in Table IV. The first 3 harmonics were assumed as measurement data. Any signal below -30dBm was discarded. There were 111 error functions in total.

ℓ_2 optimization was applied to extract the model parameters and the result is listed under column Case 2 in Table I. Fig. 4 illustrates the modeling results at a bias point other than those considered in the optimization. Excellent agreement is observed.

As for Case 1, parameters at the solution were perturbed uniformly by 20 to 40 percent and re-optimized. Of six starting points, four converged to the same solution with little variances in R_{10} and K_R. The other two converged to different points with different final objective function values.

Fig. 5 shows the characteristics of drain-to-source nonlinear current sources of the Curtice model and the modified Materka and Kacprzak model, and again we have reached an excellent match. Notice that only 6 bias points are used in the optimization which is even less than the total number of parameters for this current source. However, since we modeled under actual large-signal conditions, employing higher harmonic measurements, a much larger range of information has been covered than individual points on the DC I-V curve can provide.

Case 3: Processing Measurement Data from Texas Instruments.

Actual GaAs FET measurement data was obtained from Texas Instruments [13] including small-signal and large-signal measurements. We used the small-signal S-parameter measurement data to extract the linear parameters of the model. Large-signal measurement taken at 36 bias-input-frequency combinations was used for nonlinear parameter extraction. Table V illustrates the bias-input-frequency combinations in detail. At each combination, DC bias current and up to three RF harmonic output power measurements are available.

Optimization with the ℓ_1 norm was performed where, depending on the scales of the input and the corresponding output powers, the circuit was simulated using three to seven

harmonics. There are 20 optimization variables and 113 error functions. Among ten different starting points six converged to virtually one single solution with variations on I_{G0}, I_{B0}, α_B and R_{10} because of their relatively low sensitivities to the response functions. One typical solution is listed under the Case 3 column in Table I. Fig. 6 shows the match at the solution between the model response and measurement at one of the bias points taken into account in the optimization, while Fig. 7 shows the match at a bias point not included in the optimization. Good agreement at both bias points is observed.

Fig. 8 depicts the I-V characteristics of the drain-to-source nonlinear current source at the solution. Notice that this set of curves is obtained from large-signal parameter extraction, not from typical DC I-V curve fitting.

VI. CONCLUSIONS

An accurate and truly nonlinear large-signal parameter extraction approach has been presented, where not only DC bias and fundamental frequency, but also higher harmonic responses have been used. The harmonic balance method for nonlinear circuit simulation, adjoint analysis for nonlinear circuit sensitivity calculation and state-of-the-art optimization methods have been applied. Improvements to the convergence of the optimization process have been discussed. Numerical results have demonstrated that the method is both theoretically and computationally feasible, i.e., the method can uniquely and efficiently determine the parameters of the nonlinear elements of the GaAs MESFET model under actual large-signal operating conditions. Numerical results have also shown that under multi-bias, multi-power-input and multi-frequency excitations, spectrum measurements can effectively reflect the nonlinearities of the model and improves model reliability when used in nonlinear large-signal model parameter extraction.

Consideration of the parameter extraction problem under two-tone measurements is planned.

A computer program HarPE (Harmonic balance driven model Parameter Extractor) has been developed by Optimization Systems Associates Inc. It offers the technique presented in this paper to the microwave community through a user-friendly interface.

ACKNOWLEDGEMENTS

The authors thank Dr. R.A. Pucel of Raytheon Company, Lexington, MA, for suggesting the numerical example of Case 2. They thank Dr. A.M. Pavio of Texas Instruments, Dallas, TX, for several detailed discussions and providing experimental data to test our algorithm. They also thank Dr. R.M. Biernacki of Optimization Systems Associates Inc., Dundas, Ontario, Canada, for helpful technical discussions and suggestions.

REFERENCES

[1] Y. Tajima, B. Wrona and K. Mishima, "GaAs FET large-signal model and its application to circuit designs", *IEEE Trans. Electron Devices*, vol. ED-28, 1981, pp. 171-175.

[2] A. Materka and T. Kacprzak, "Computer calculation of large-signal GaAs FET amplifier characteristics", *IEEE Trans. Microwave Theory Tech.*, vol. MTT-33, 1985, pp. 129-135.

[3] J.W. Bandler, S.H. Chen, S. Ye and Q.J. Zhang, "Integrated model parameter extraction using large-scale optimization concepts", *IEEE Trans. Microwave Theory Tech.*, vol. MTT-36, 1988, pp. 1629-1638.

[4] W.R. Curtice, "GaAs MESFET modeling and nonlinear CAD", *IEEE Trans. Microwave Theory Tech.*, vol. MTT-36, 1988, pp. 220-230.

[5] M.A. Smith, T.S. Howard, K.J. Anderson and A.M. Pavio, "RF nonlinear device characterization yields improved modeling accuracy", *IEEE Int. Microwave Symp. Digest* (Baltimore, MD), 1986, pp. 381-384.

[6] M. Paggi, P.H. Williams and J.M. Borrego, "Nonlinear GaAs MESFET modeling using pulsed gate measurements", *IEEE Int. Microwave Symp. Digest* (New York, NY), 1988, pp. 229-231.

[7] B. Kopp and D.D. Heston, "High-efficiency 5-Watt power amplifier with harmonic tuning", *IEEE Int. Microwave Symp. Digest* (New York, NY), 1988, pp. 839-842.

[8] U. Lott, "A method for measuring magnitude and phase of harmonics generated in nonlinear microwave two-ports", *IEEE Int. Microwave Symp. Digest* (New York, NY), 1988, pp. 225-228.

[9] K.S. Kundert and A. Sangiovanni-Vincentelli, "Simulation of nonlinear circuits in the frequency domain", *IEEE Trans. Computer-Aided Design*, vol. CAD-5, 1986, pp. 521-535.

[10] J.W. Bandler, Q.J. Zhang and R.M. Biernacki, "A unified theory for frequency-domain simulation and sensitivity analysis of linear and nonlinear circuits", *IEEE Trans. Microwave Theory Tech.*, vol. MTT-36, 1988, pp. 1661-1669.

[11] *Microwave Harmonica User's Manual*, Compact Software Inc., Paterson, NJ, 07504, 1987.

[12] J.W. Bandler, S.H. Chen and S. Daijavad, "Microwave device modeling using efficient ℓ_1 optimization: a novel approach", *IEEE Trans. Microwave Theory Tech.*, vol. MTT-34, 1986, pp. 1282-1293.

[13] Measurement data provided by Texas Instruments, Dallas, TX, Jan. 1989.

[14] P. Rabinowitz, *Numerical Methods for Nonlinear Algebraic Equations*. New York: Gorden and Breach Science Publishers, 1970, pp. 87-161.

[15] J.W. Bandler, Q.J. Zhang, and R.M. Biernacki, "Practical, high speed gradient computation for harmonic balance simulators", *IEEE Int. Microwave Symp. Digest* (Long Beach, CA), 1989.

TABLE I

PARAMETER VALUES OF THE INTRINSIC PART OF THE MODIFIED MATERKA AND KACPRZAK FET MODEL

		Value		
Name	Unit	Case 1	Case 2	Case 3
I_{DSS}	A	0.1888	0.0521	0.0740
V_{P0}	V	-4.3453	-1.267	-3.185
γ	-	-0.3958	-0.0877	0.0177
E	-	2.0	1.269	2.937
K_E	1/V	0.0	-0.3224	-0.9077
S_1	1/Ω	0.0972	0.0731	0.1527
K_G	1/V	-0.1678	-0.6482	-0.4912
τ	pS	3.654	5.322	0.1011
S_s	1/Ω	0.0	4.462×10^{-5}	0.0022
I_{G0}	A	0.5×10^{-9}	8.782×10^{-9}	4.965×10^{-11}
α_G	1/V	20.0	34.04	20.32
I_{B0}	A	0.5×10^{-9}	5.960×10^{-12}	1.000×10^{-12}
α_B	1/V	1.0	4.245	2.000
V_{BC}	V	0.0*	20.0*	20.0*
R_{10}	Ω	4.4302	0.0361	0.1243
K_R	1/V	0.0	9.892×10^{-3}	0.0
C_{10}	pF	0.6137	1.066	1.170
K_1	1/V	0.7686	1.531	1.201
C_{1S}	pF	0.0	0.0314	-0.5243
C_{F0}	pF	0.0416	1.321	0.0623
K_F	1/V	0.0	1.638	-0.0959

* the value is fixed during the optimization

TABLE II

MATCH ERRORS BETWEEN THE MEASUREMENTS AND MODEL RESPONSES IN CASE 1

	P_{out} matching errors in (%)		
Harm. Match	(H=1)	(H=2)	(H=3)
First harm.	-0.53	-0.84	-1.08
Second harm.	21.32	7.58	6.77
Third harm.	-37.48	-14.36	-9.31

where H=1, 2, or 3 corresponds to the number of harmonics included in the objective function (3), and the comparisons here are made at bias point (V_{GB}=-2V, V_{DB}=2V), available input power P_{in}=10dBm and fundamental frequency f_1=1GHz.

TABLE III

PARAMETERS OF THE CURTICE MODEL USED IN CASE 2

Parameter	β_2 (1/V)	A_0 (A)	A_1 (A/V)	A_2 (A/V^2)
Value	0.04062	0.05185	0.04036	-0.009478
Parameter	A_3 (A/V^3)	γ (1/V)	V_{DS0} (V)	I_S (A)
Value	-0.009058	1.608	4.0	1.05×10^{-9}
Parameter	N (-)	C_{GS0} (pF)	C_{GD0} (pF)	F_C (-)
Value	1.0	1.1	1.25	0.5
Parameter	G_{MIN}(1/Ω)	V_{BI} (V)	V_{BR} (V)	τ (ps)
Value	0.0	0.7	20	5.0

see [4]

TABLE IV

INPUT LEVELS USED WITH DIFFERENT FUNDAMENTAL FREQUENCIES AND DIFFERENT BIASES IN CASE 2

(V_{GB}, V_{DB})	P_{in} (dBm)			
	f_1=0.5GHz	f_1=1.0GHz	f_1=1.5GHz	f_1=2.0GHz
(-0.3, 3)	0, 4	0, 4	0, 4	0, 4
(-0.3, 7)	0, 4	0, 4	0, 4	0, 4
(-1.0, 3)	0	0	0	0
(-1.0, 7)	0	0, 4	0, 4	0
(-0.5, 3)	--	8	8	--
(-0.5, 7)	8	8	8	8

f_1 denotes the fundamental frequency

TABLE V

BIAS-INPUT-FREQUENCY MEASUREMENT COMBINATIONS FOR THE NUMERICAL EXAMPLE OF CASE 3

	P_{in} = -15, -10, -5, 0, 5, 10 dBm		
	f_1=0.2GHz	f_1=6.0GHz	f_1=10GHz
Bias 1	(-0.373,2)	(-0.372,2)	(-0.372,2)
Bias 2	(-1.072,6)	(-1.073,6)	(-1.069,6)

where f_1 means fundamental frequency and the number pairs in the brackets are the bias voltages (V_{GB},V_{DB})

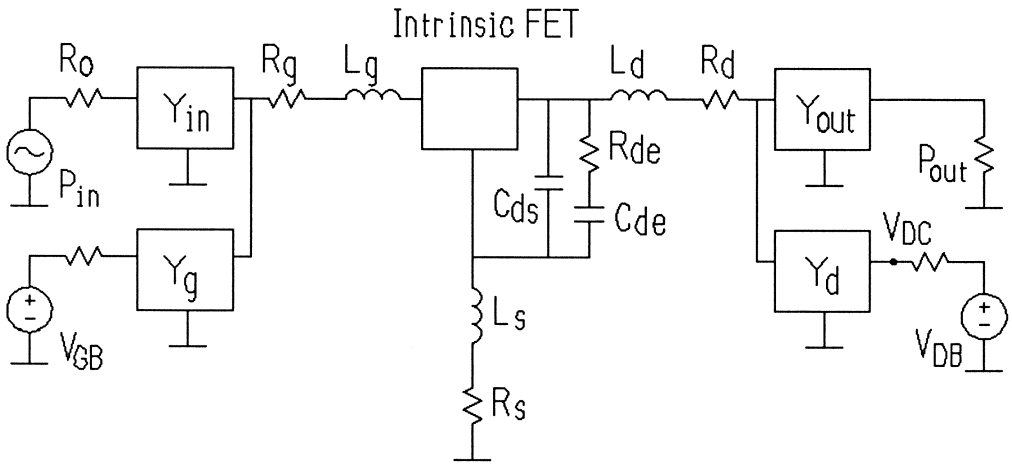

Fig. 1 Circuit setup for large-signal multi-harmonic FET measurement.

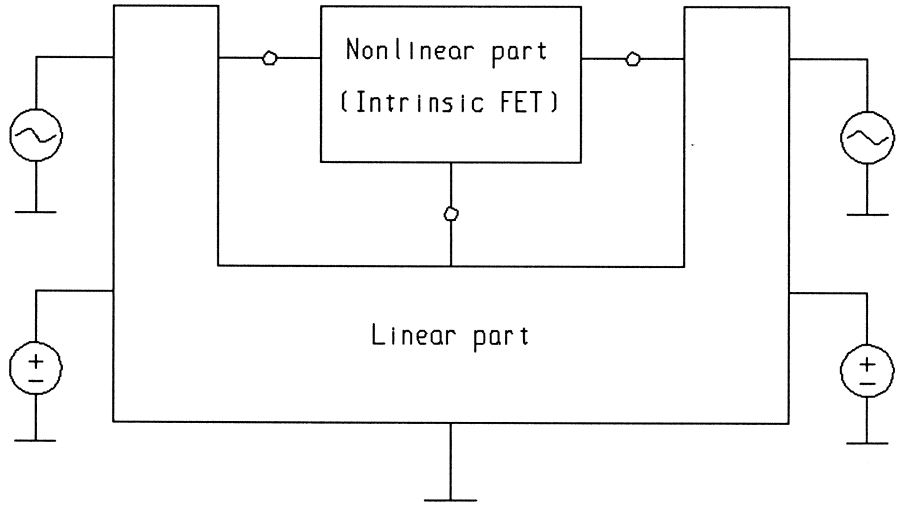

Fig. 2 Block diagram for illustrating circuit simulation using the harmonic balance method.

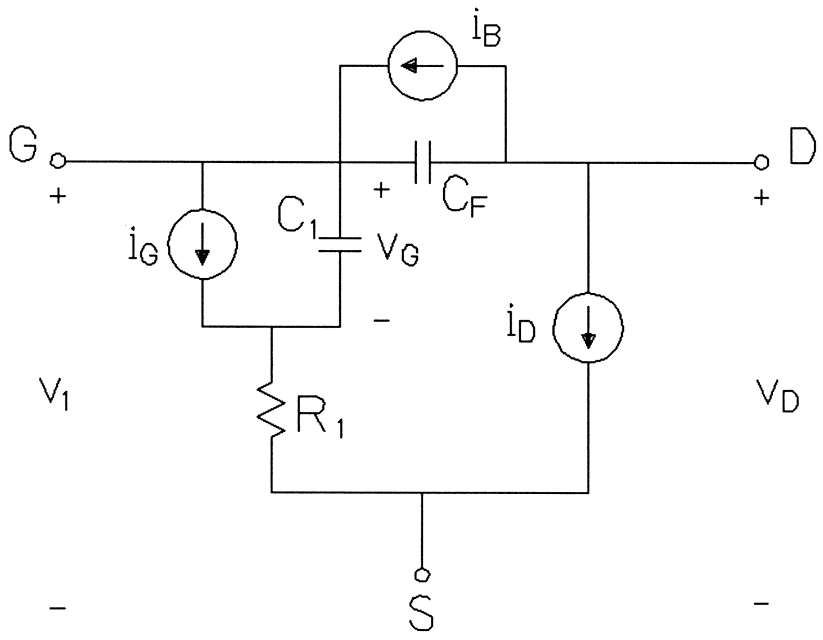

Fig. 3 Intrinsic part of the modified Materka and Kacprzak FET model.

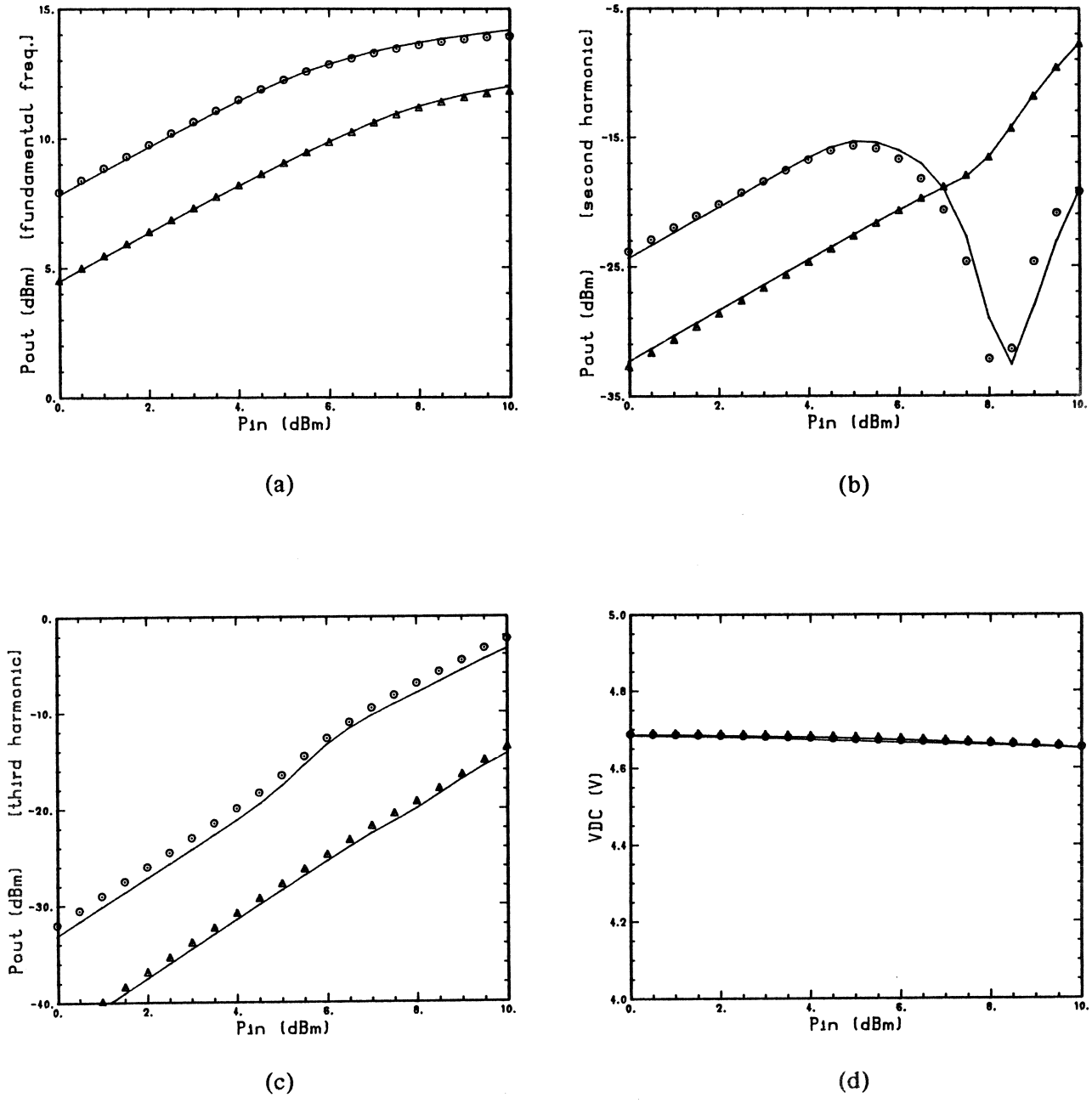

Fig. 4 Agreement between the (Materka) model response and the simulated measurements (using the Curtice model) at V_{GB}=-0.5 and V_{DB}=5 in Case 2. Solid lines represent the (Materka) computed model response. Circles denote the simulated measurements at fundamental frequency 0.5GHz and triangles the simulated measurements at fundamental frequency 1.5GHz. (a) Fundamental component, (b) second harmonic component, (c) third harmonic component, and (d) DC component.

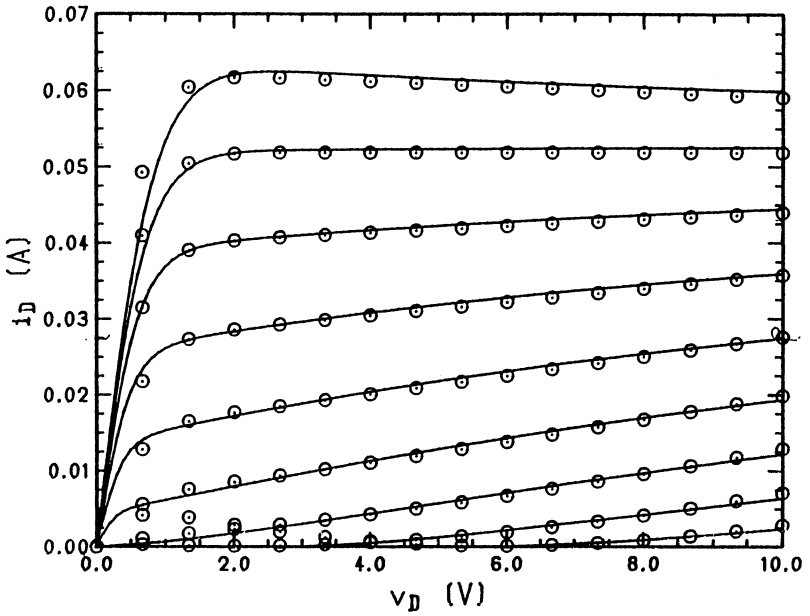

Fig. 5 Agreement between the DC characteristics of the modified Materka and Kacprzak model and the simulated measurements (from the Curtice model) in Case 2. V_G is from -1.75V to 0.25V in steps of 0.25V, and V_D is from 0 to 10V. (Curtice uses V_{in} and V_{out}, respectively.) Solid lines represent the (Materka) model, and the circles represent the measurements.

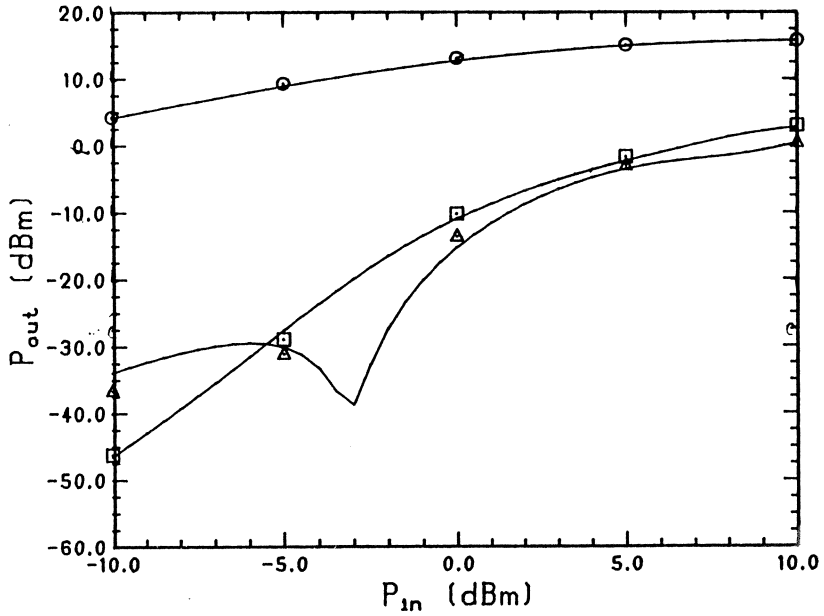

Fig. 6 Agreement between the (Materka) model responses and the measurements from Texas Instruments at fundamental frequency 0.2GHz, and bias point V_{GB}=-0.373V and V_{DB}=2V. (This bias point has been included in the optimization.) Solid lines represent computed model responses. Circles, triangles and squares denote fundamental, second and third harmonic measurements, respectively.

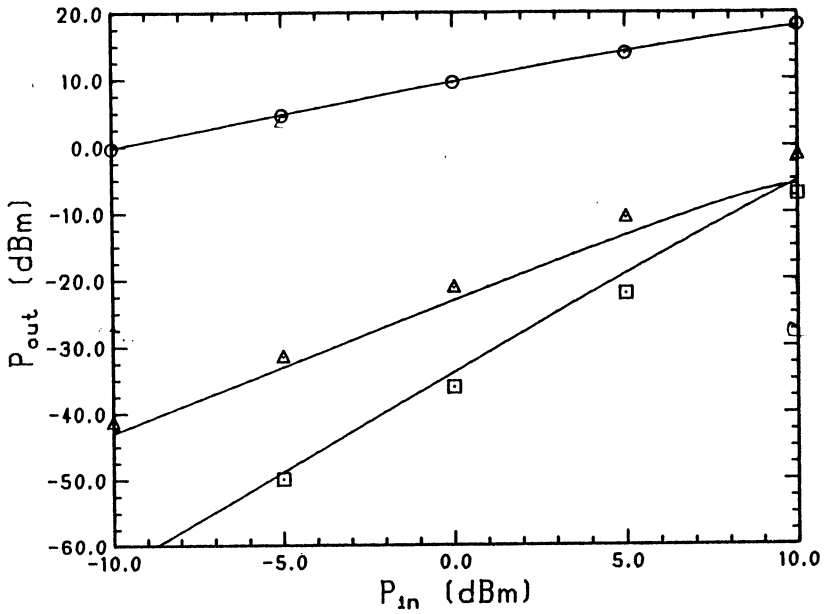

Fig. 7 Agreement between the (Materka) model response and the measurements from Texas Instruments at fundamental frequency 6GHz, and bias point V_{GB}=-0.673V and V_{DB}=4V. (This bias point has not been included in the optimization.) Solid lines represent computed model responses. Circles, triangles and squares denote fundamental, second and third harmonic measurements, respectively.

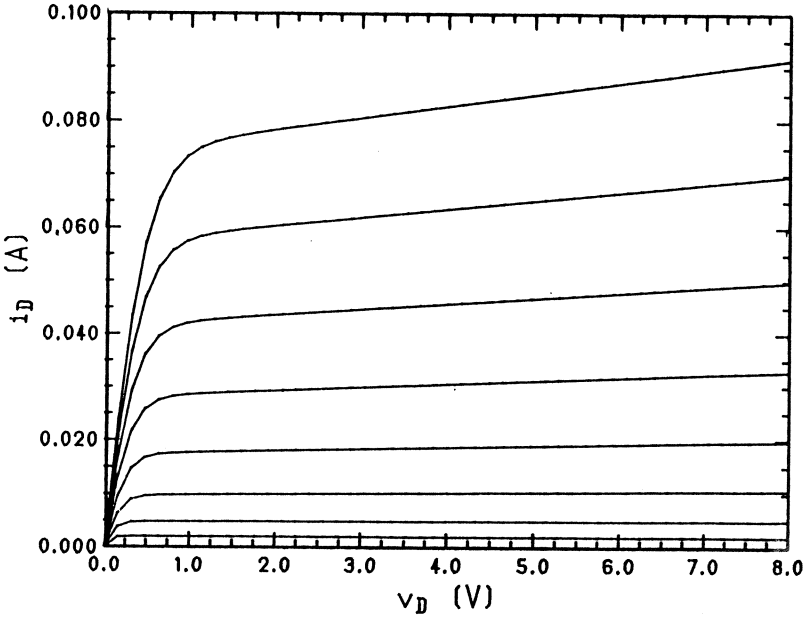

Fig. 8 DC characteristics of the drain-to-source nonlinear current source of the modified Materka and Kacprzak model after the optimization to match the large-signal measurement data provided by Texas Instruments. V_G is from -1.75V to 0.25V in steps of 0.25V, and V_D is from 0 to 10V.